Journal of *Marine Science and Engineering*

MDPI

Article

The Construction and Application of Dual-Objective Optimal Speed Model of Liners in a Changing Climate: Taking Yang Ming Route as an Example

Jinxing Lu [1], Xianhua Wu [1,2,*] and You Wu [3]

[1] School of Economics and Management, Shanghai Maritime University, Shanghai 201306, China
[2] Collaborative Innovation Center on Climate and Meteorological Disasters, Nanjing University of Information Science & Technology, Nanjing 210044, China
[3] Earth System Science Interdisciplinary Center, University of Maryland, College Park, MD 20740, USA
* Correspondence: 185390@shmtu.edu.cn; Tel.: +86-(21)-38282475

Abstract: In a changing climate, ship speed optimization plays an important role in energy conservation and emission reduction. In order to establish a dual-objective optimization model of minimizing ship operating costs and reducing carbon emissions, fuel costs, berthing costs, emission costs and fixed cost during sailing cycles, the emission reduction strategies of ships using MGO in emission control areas and the AMP in ports are taken into account. The PSO algorithm is adopted to find the Pareto solution set, and the TOPSIS algorithm is used to screen the optimal compromise solution, while Yang Ming, a trans-Pacific route, is selected to verify the applicability of the model. The result shows that the optimization model can effectively reduce the operating cost during sailing cycles and control carbon emissions, which can provide references for ship operation decision-making to achieve carbon peaking and carbon neutrality.

Keywords: dual-objective optimal speed; carbon peaking and carbon neutrality; emission control area; PSO algorithm; TOPSIS algorithm; Yang Ming route

Citation: Lu, J.; Wu, X.; Wu, Y. The Construction and Application of Dual-Objective Optimal Speed Model of Liners in a Changing Climate: Taking Yang Ming Route as an Example. *J. Mar. Sci. Eng.* **2023**, *11*, 157. https://doi.org/10.3390/jmse11010157

Academic Editor: Theocharis D. Tsoutsos

Received: 16 December 2022
Revised: 27 December 2022
Accepted: 29 December 2022
Published: 9 January 2023

1. Introduction

Carbon emissions are the main cause of global warming. The transportation industry is one of the major sources of carbon emissions. The data from the International Energy Agency showed that the carbon dioxide emitted by the transportation industry accounted for 24% in 2019 (Figure 1). According to the report from Simpson Spence & Young (SSY), a shipping consulting firm, the carbon dioxide emissions of the global shipping industry were 794 million tons in 2020, accounting for 2.4% of the global total carbon emissions, and the carbon dioxide emissions of the global shipping industry were of 833 million tons in 2021, accounting for 3% of the global total carbon emissions, with a yearly increase 4.9%. Shi et al. (2020) thought that the pollution caused by fuel consumption during the voyage could not be ignored, and those pollutants may also have negative impacts on public health and global climate change [1]. Wu et al. (2022) pointed out the significant negative impact of air pollution on residents' living welfare [2,3]. Therefore, it is urgent to reduce carbon emissions in the transportation industry.

In addition, the international community is also paying attention to green shipping. In order to control the air pollution caused by ships, the International Maritime Organization issued the MARPOL Convention, Annex VI in 2008, establishing SOx Emission Control Areas (hereinafter referred to as SECAs). There is a strict requirement on the sulfur content of fuel in the ECA, e.g., after 1 July 2010, the sulfur content of the SECAs was less than 1%m/m. After 1 January 2015, the sulfur content was less than 0.1%m/m. In addition, IMO also proposed some non-mandatory emission reduction measures, such as using alternative marine power (hereinafter referred to as AMP), optimizing shipping routes, improving

shipping efficiency, strengthening ship equipment management, etc. The use of energy on the ship's main engine will simultaneously emit polluting gases such as SO_2 and CO_2, as a high correlation exists between SO_2 and CO_2 emissions.

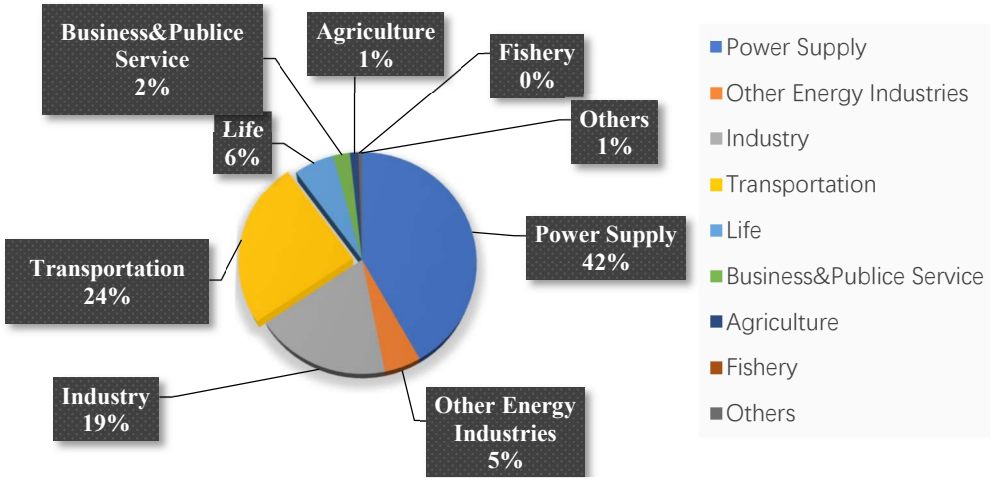

Figure 1. Proportions of global carbon emissions by sector in 2019.

At the same time, in order to improve the energy efficiency of existing ships and achieve the preliminary strategic goal of greenhouse gas emission reduction set by IMO, mandatory requirements for the existing Ship Energy Efficiency Index (EEXI), carbon intensity Index (CII) and Ship Energy Efficiency Management Program (SEEMP) were put forward at the 76th session of the Commission for Marine Environmental Protection. For the moment, there are a few studies on the optimization of CO_2 emissions in the SECAs. For example, Jing et al. (2021) used the system dynamics model and set 12 scenarios with different fuel use conditions and ship speeds to investigate the trend of carbon dioxide emissions in the Northern Sea Route [4]. Xu and Yang (2020) showed that the use of LNG-fueled container ships through the Northern Passage saves costs and reduces CO_2 emissions [5]. However, these studies are different from this paper. First of all, in terms of research content, this paper takes the route of Yang Ming as an example to optimize the ship speed with the dual objectives of minimizing the total operating cost and minimizing the CO_2 emissions of the ship. Secondly, in terms of research methods, this paper uses the multi-objective particle swarm optimization (hereinafter referred to as MOPSO) algorithm to obtain the Pareto front, and the TOPSIS algorithm to obtain the best compromise solution. Therefore, this study has its particularity and will enrich the research on carbon dioxide emissions in SECAs.

At present, under the background of depressed freight rates in the shipping market, cost control will be one of the important goals of shipping companies. Nevertheless, in order to reach the emission standards in the routes passing through the SECAs, the common methods are to use the standard fuel oil or install desulfurization devices on the ships already in operation, but these two methods will increase the operating costs of the ships. A desulfurized device costs millions of USD, which is a large expense for a shipping company. Therefore, in the context of low carbon, how to control the cost has become the focus of shipping companies. According to the China Maritime Service Network (www.cnss.com accessed on 25 June 2022.) which shows the prices of marine fuel oil (hereinafter referred to as MFO) and marine gas oil (hereinafter referred to as MGO), in the Singapore Port from April 2022 to September 2022 (Figure 2), the average price of MFO was USD 597.1 per ton, while the average price of MGO was as high as USD 1153.7 per ton, which was about twice the MFO's price. Using MGO would significantly increase the operating cost of ships while meeting the emission standard. Meanwhile, reducing the speed and using new ships that meet the standards are the main ways to achieve the greenhouse gas emission reduction target and meet the relevant indicators of EEXI, CII and SEEMP. Reducing speed

can not only effectively reduce fuel consumption and lower fuel cost, but also reduce carbon emissions. However, reducing speed will extend the sailing cycle and increase the operating cost. If a ship accelerates to shorten the sailing cycle, it will increase carbon emissions. In addition, the direct use of new ships that meet the standards will reduce carbon emissions, but the cost will be greatly increased. Therefore, the purpose of this paper is to identify how to determine the speed in/out of ECA for ships to reach a balance between reducing both costs and CO_2 emissions to achieve the dual objectives of protecting the environment and saving costs.

Figure 2. Prices of MFO and MGO in Singapore Port in 2022.

2. Literature Review

Currently, the objectives of most speed optimization models are to either minimize sailing costs or maximize profits. For example, Lin Guihua et al. (2022) established an optimization model to maximize profits by considering some comprehensive emission reduction strategies in control areas and simultaneously taking into account the revenue of carriers and various costs during the voyage [6]. Given the optimization of ship deployment, route, speed and fueling, Lashgari et al. (2021) developed a stochastic linear integer programming model based on scenarios to effectively reduce total costs [7]. With the total fuel consumption as the objective function and the main engine speed as the decision variable, Fan et al. (2021) established a multiple-stage speed optimization model of ships based on a dynamic programming algorithm [8]. Li et al. (2020) comprehensively took into account the impact of sea state and voluntary speed loss on sailing and established a single-voyage optimization model to minimize the main engine fuel consumption and ship operating cost [9]. In order to optimize the allocation of multi-route and multi-type liner routes and take into account sailing speed and ship payload, Gao and Hu (2021) established a multi-objective mixed integer nonlinear optimization model [10]. With the objective of minimizing the total costs of the fleet including operating cost, capital cost and sailing cost, Wang and Zhao (2021) solved the model by applying an algorithm based on probabilistic taboo search [11]. Yu et al. (2019) established a dual-objective optimization model with the objectives of optimizing sailing cost and shipper satisfaction and adopted a fuzzy membership function in the model to represent the satisfaction of shippers [12]. Doudnikoff and Lacoste (2014) established an optimization model to minimize the cost without adding new ships, and they concluded that the increase in speed outside the emission control zone would slightly reduce the total cost, but increase CO_2 emissions [13]. Ng (2019) considered the relationship between sailing speed and the number of ships required to maintain a given service frequency and established a new sailing speed optimization model, which can greatly shorten the calculation time and improve the calculation efficiency [14]. De et al. (2021) studied the optimal management strategy under different fuel pricing modes with the goal of minimizing the total cost [15]. De et al. (2017) considered the concept of time

window constraints and proposed a model for solving shipping inventory paths, which is helpful for shipping companies to reduce the total cost [16].

Carbon reduction strategy is one of the main marine topics of the last decade. Dulebenets (2018) introduced the carbon tax cost, considered the CO_2 emissions of ships in the states of sailing and berthing, respectively, and studied route ship allocation and speed optimization in ECA [17]. Thalis (2014) indicated that the use of AMP could reduce CO_2 emissions by 48–70% when docked [18]. Meanwhile, Tang et al. (2018) indicated that minimal emissions were produced in ports with power supplied from clean energy [19]. Lan et al. (2020) considered the impact of carbon emissions trading policies on ship operation, established speed optimization models under four different forms of carbon emission policies and compared the impacts of carbon emission trading policies and carbon emission tax on ship carbon emissions and ship operating cost. Their results showed that the carbon emission tax had a better emission reduction effect than that of carbon emissions trading policies, while carbon emission trading policies had a smaller impact on the profits of shipping companies [20]. De et al. (2016) proposed an optimization model that included multiple time windows, carbon emissions and the needs of different ports [21]. Ding et al. (2020) investigated the economic impact of fixed carbon emission tax rate and progressive carbon emission tax rate on the Arctic Route. The results showed that both solutions would increase sailing costs and reduce ship profits. However, progressive carbon emission tax produced a smaller cost, which was easy to be adopted by shipping companies [22]. De et al. (2020) took carbon emission reduction as the main goal and studied the sustainable ship route optimization of ship fuel management [23]. On the basis of considering the upper limit of carbon emissions and carbon emission tax, Xing et al. (2019) established a mixed integer nonlinear programming model of ship speed and fleet allocation and analyzed the impacts of various carbon tax and carbon emission upper limits on ship speed and route ship allocation [24]. De et al. (2021) discussed a model that maximizes shipping companies' profits by combining fuel consumption and carbon emissions [25].

There are also many studies on the impact of non-mandatory carbon emission reduction policies on ship carbon emissions and ship operating costs. Aiming at the scheduling problem of tramp ships including speed optimization, Fan et al. (2019) established a multi-type tramp ship scheduling and speed optimization model considering carbon emissions with the goal of minimizing the total cost of shipping companies [26] without establishing a double-objective optimization model. Zhen et al. (2020) established a dual-objective optimization model to minimize fuel costs and SO_2 emissions and verified that ECA rules could effectively reduce SO_2 emissions from ships [27] without consideration of non-mandatory emission reduction policies. Christodoulou et al. (2019) collected the various initiatives developed and implemented to reduce maritime air emissions that are fully implemented globally [28]. Liu et al. (2016) studied CO_2 emissions from shipping in East Asia based on detailed ship dynamic activity data, showing that emissions from shipping in East Asia accounted for 16% of global CO_2 emissions in 2013 [29]. Burel et al. (2013) proposed the economic upturn that could be achieved by using LNG as a fuel for merchant ships. A case study shows that LNG reduces operating costs by 35% and CO_2 emissions by 25% [30]. Ju and Hargreaves (2021) conducted a comprehensive analysis of CO_2 emissions in the western Singapore Strait based on voyage data from the Automatic Identification System and static information from the Singapore Maritime Data Centre [31].

Undoubtedly, a number of studies are relevant to ship carbon emissions and ship operating costs. Few papers discussed the optimization model of ship speed based on the comprehensive consideration of the ECA, the use of AMP and the proposal of carbon emission trading price to meet the relevant indicators such as CII, as well as the establishment of the ship speed optimization with the minimum carbon emissions and the minimum operating costs. Therefore, this paper has carried on the research work in the navigation speed optimization, slow sailing and other aspects. This paper takes Yang Ming, a trans-Pacific shipping route, as an example, considering ECA, AMP, carbon trading price and other factors. Simultaneously, fuel cost, berthing cost, emission cost and fixed cost

during sailing cycles are taken into account. We establish a dual-objective optimization model of minimizing operating cost and minimizing carbon emissions during sailing cycles, adopt the MOPSO method to solve the Pareto solution set and use TOPSIS to screen the optimal compromise solution and offer the optimal solution. This paper provides a better path for a speed optimization model for the route involving emission control areas and aiming at minimizing carbon emission and ship operating cost. These are the focus of this paper, and also the differences between this paper and current studies.

3. Problem Description and Model Establishment

3.1. Problem Description and Hypothesis

Liner carriers transport cargoes for customers at the ports along the routes on a regular basis each week. In order to reduce operating cost during the cycles as much as possible and reduce ship pollutant emissions as far as possible, liner carriers should use MGO in SECAs; in addition, when docked in ports, AMP must be used. Ship operating cost mainly consists of fuel cost, emission cost, berthing cost and fixed cost. Ship speed reduction will reduce fuel consumption, ship emissions, fuel cost and emissions cost. However, it will simultaneously increase sailing time and operating cost. Therefore, reducing ship emissions and reducing operating costs are in conflict. v_i is the decision variable. Q_{AMP}, B_j^{AMP}, P_j^{AMP}, P_{CO_2}, n and C_g are parameters. The variables and parameters are shown in Table 1.

Table 1. Variables and parameters.

Variable and Parameter	Meaning
$I = \{i \mid i \in Z^*\}$	Set of legs, that is to say, the path between two neighboring ports
$J = \{j \mid j \in Z^*\}$	Set of ports
t_i^E, t_i^N	Time of leg i in/outside SECAs (h)
P_E, P_N	Fuel prices in/outside SECAs (USD/t)
F_Z, F_F, F_{FS}	Daily fuel consumption of the main engine during the voyage, auxiliary engines during the voyage and auxiliary engines when docked (t/d)
Q_{AMP}	Daily average demand volume of AMP by each ship when docked
P_j^{AMP}	Price of AMP used in port j (USD/kWh)
B_j^{AMP}	Subsidy for the use of AMP in port j (USD/cycle)
t_j	Time of berthing in port j (h)
P_{CO_2}	Carbon emissions trading price (USD/t)
n	Number of ships within a cycle
$f_{co_2}^E, f_{CO_2}^N$	Emission factors of carbon dioxide in/outside SECAs
C_g	Daily fixed cost of ships, excluding berthing cost (USD/d)
v_i	$v_i = \{v_i^E, v_i^N\}$, ship speed for leg i in/outside SECAs

Hypotheses in this paper:

(1) MGO is used by the main engine in the SECAs and MFO is used outside the SECAs, and MGO is always used by the auxiliary engines;
(2) The ship speed is constant in different areas for leg i;
(3) The service frequency of ships is once a week;
(4) The type of ships for the route is the same, with the same capacity and cost structure;
(5) The ships sail at constant speed in SECAs. The ships sail at constant speed outside SECAs;
(6) In ports equipped with AMP, all ships use AMP when docked.

3.2. Objective Function

3.2.1. Fuel Cost

Each leg is divided into in/outside SECAs and the total fuel costs of all main engine and auxiliary engines of the ship during one cycle are:

$$C_R = C_{ZR} + C_{FR} \tag{1}$$

The study of Hughes (1996) indicated that the fuel consumption of the ship was proportional to the cube of speed [32]. Therefore, the daily fuel consumption F_Z of the main engine during the voyage of the ship is:

$$F_Z(v_i) = q_Z \times EL_Z \times P_Z \times \frac{24}{10^6} = q_Z \times EL_Z \times P_0 \times \left(\frac{v_i}{v_0}\right)^3 \times \frac{24}{10^6} \quad (2)$$

Among them, the fixed value of the main engine load value EL_Z is 0.8, q_z refers to the fuel consumption rate (g/kWh), P_0 refers to the rated main engine power, V_0 refers to the ship's design speed and P_z refers to the actual main engine power. f_0^Z, the fuel consumption coefficient, will be introduced by calculating fuel consumption. When calculated based on the standard ship with a capacity of 5000 TEU, f_z = 0.0108, the fuel formula of the main engine is:

$$f_z = q_Z \times EL_Z \times P_0 \times \frac{24}{(v_0)^3 \times 10^6} \quad (3)$$

Then, $F_Z(v_i) = f_0^z \times \left(v_i^E\right)^3 + f_0^z \times \left(v_i^N\right)^3$. Therefore, the total fuel costs of the main engine of the ship during one cycle are:

$$C_{ZR}(v_r) = n \times \sum_{i=1}^{I} \left\{ \frac{t_i^E}{24} \times P_E \times f_z \times \left(v_i^E\right)^3 + \frac{t_i^N}{24} \times P_N \times f_z \times \left(v_i^N\right)^3 \right\} \quad (4)$$

The daily fuel consumption by auxiliary engines when ships sail in/outside SECAs is:

$$F_F = q_F \times EL_F \times P_0 \times \frac{24}{10^6} \quad (5)$$

Among them, the fixed value of the auxiliary engine load value EL_F is 0.5. q_F refers to the fuel consumption rate (g/kWh), P_0 refers to the rated auxiliary engine power. The fuel consumption of auxiliary engines is correlated to the ship and the performance of its engines, and it is not influenced by speed. Therefore, the total fuel costs of all auxiliary engines of the ship during one cycle are:

$$C_{FR} = n \times \sum_{i=1}^{I} P_E \times \frac{t_i}{24} \times F_F \quad (6)$$

Then, the total fuel costs of all main engine and auxiliary engines of the ship during one cycle are:

$$\begin{gathered} C_R = C_{ZR} + C_{FR} \\ = n \times \sum_{i=1}^{I} \left\{ \frac{t_i^E}{24} \times P_E \times f_0^z \times \left(v_i^E\right)^3 + \frac{t_i^N}{24} \times P_N \times f_0^z \times \left(v_i^N\right)^3 + P_N \times \frac{t_i}{24} \times F_F \right\} \end{gathered} \quad (7)$$

3.2.2. Berthing Cost

The berthing cost is divided into two types by using AMP or not. If AMP is used when the ship is docked, it mainly consumes power. Additionally, currently the country is actively promoting the use of AMP, offering corresponding subsidies to line carriers. Therefore, the berthing cost when using AMP is:

$$C_S = \sum_{j=1}^{J} n \times \left(\frac{t_j}{24} P_j^{AMP} Q_{AMP} - B_j^{AMP} \right) \quad (8)$$

If AMP is not used, then the fuel when docked is consumed by auxiliary engines, and in this case the berthing cost is:

$$C_S = \sum_{j=1}^{J} n \times \frac{t_j}{24} \times F_{FS} \times P_E \quad (9)$$

3.2.3. Emission Costs

The emission costs consist of those produced during the voyage and when docked. Xue (2014) suggested that, during the voyage, the fuel consumed by the main engine of a container ship accounted for 87%, the auxiliary engines 11% and the boilers in operation approximately 2%; thus, we did not consider the emissions produced by boilers [33]. The emission cost during the voyage is generated from fuel consumption. When docked, it only needs to consider fuel consumption by auxiliary engines, without considering the power consumption caused by the use of AMP. Then, when AMP is used, the carbon dioxide emissions are:

$$F_{CO_2} = n \times \sum_{i=1}^{I} \left\{ \frac{t_i^E}{24} f_{co_2}^E f_0^z \left(v_i^E\right)^3 + \frac{t_i^N}{24} f_{co_2}^N f_0^z \left(v_i^N\right)^3 + f_{co_2}^N \frac{t_i}{24} F_F \right\} \tag{10}$$

If AMP is not used, the carbon dioxide emissions are:

$$F_{CO_2} = n \sum_{i=1}^{I} \left\{ \frac{t_i^E}{24} f_{co_2}^E f_0^z \left(v_i^E\right)^3 + \frac{t_i^N}{24} f_{co_2}^N f_0^z \left(v_i^N\right)^3 + f_{co_2}^N \frac{t_i}{24} F_F \right\} + n \sum_{j=1}^{J} \left\{ \frac{t_j}{24} F_{FS} f_{CO_2}^E \right\} \tag{11}$$

The emission cost is equal to the product of emission F_{CO_2} and the carbon dioxide emissions trading price P_{CO_2}. The carbon dioxide emissions trading price is based on the international trading price of USD 47/ton. Therefore, all emission costs during the entire cycle are:

$$C_{CO_2}\left(v_i^E, v_i^N\right) = P_{CO_2} \times F_{CO_2} \tag{12}$$

3.2.4. Fixed Cost

In liner shipping, besides cost, emission cost, berthing cost and other variable costs, some fixed costs are also included, which are mainly insurance cost, repair cost, management cost, etc. There are also some variable costs including port charges and handling charges which are not related to speed and pollutant emissions. In order to simplify the study, the costs are uniformly referred to as fixed costs here.

$$C_G = n \times \frac{1}{24} \times C_g \times \left(\sum_{i=1}^{I} t_i + \sum_{j=1}^{J} t_j \right) \tag{13}$$

3.3. Construction of Dual-objective Optimization Model

With the dual objectives of minimizing the costs and carbon emissions of liner carriers, the following model can be established, which mainly includes the objective function and constraints.

$$minTC\left(v_i^E, v_i^N\right) = C_R\left(v_i^E, v_i^N\right) + C_S + C_{CO_2}\left(v_i^E, v_i^N\right) + C_G\left(v_i^E, v_i^N\right) \tag{14}$$

$$minF_{CO_2}\left(v_i^E, v_i^N\right) = F_{CO_2}\left(v_i^E, v_i^N\right) \tag{15}$$

$$s.t.\ V_m < v_i^E, v_i^N < V_M, \forall i \in I \tag{16}$$

$$t_i^N = \frac{L_i^N}{v_i^N}, t_i^E = \frac{L_i^E}{v_i^E}, t_i = t_i^N + t_i^E \tag{17}$$

$$\sum_{i=1}^{I} t_i + \sum_{j=1}^{J} t_j \le 168 \times n \tag{18}$$

$$i = 1, 2, \ldots, i; j = 1, 2, \ldots, j; n = 1, 2, \ldots, n \tag{19}$$

The objective function (14) refers to the minimum transport cost of the liner company. $C_R\left(v_i^E, v_i^N\right)$ refers to the fuel cost during the voyage; C_S refers to the berthing cost; $C_{co_2}\left(v_i^E, v_i^N\right)$ refers to the carbon dioxide emission cost; $C_G\left(v_i^E, v_i^N\right)$ refers to the fixed cost of one voyage of the ship; objective function (15) refers to the total carbon dioxide emissions during one voyage of the ship.

Constraint (16) refers to the speed limit of the ship, specifying a speed between the minimum speed and the design speed; constraint (17) means that time is equal to the identical equation for the distance divided by the speed; constraint (18) refers to the service frequency of the ship visiting the port at least once a week; constraint (19) refers to the non-negative and integer constraints on the number of legs, ports and ships. To solve the above-mentioned optimization model, the dual-objective optimization algorithms and solution ideas are introduced below.

4. Dual-Objective Optimization Algorithms and Solutions

4.1. Particle Swarm Optimization

4.1.1. Basic Principle of the Algorithm

De et al. (2019) proposed a multi-objective mathematical model integrating different shipping services and used multi-objective particle swarm optimization algorithm and non-dominated sorting genetic algorithm to solve the model [34]. Peng et al. (2021) adopted the MOPSO algorithm to solve the multi-objective model of berth allocation for arriving ships [35].Mandal and Mondal (2021) applied the MOPSO–TOPSIS algorithm to solve the multi-objective model and obtained the optimal solution [36]. Therefore, the multi-objective particle swarm optimization algorithm is used in this paper. Based on the idea of Birds' foraging behavior, Kennedy and Eberhart (2002) proposed the PSO Algorithm [37]. The development of the MOPSO algorithm was relatively late [38]. Through Pareto ranking approaches, MOPSO uses the dominant relationship of fitness among particles to find the individual optimal solution set and swarm optimal solution set and update the non-inferior solution set to solve the multi-objective problem.

For a particle swarm the size of N, the position vector x_i and velocity vector v_i of any particle i are, respectively, expressed as:

$$x_i = (x_{i1}, x_{i2}, \ldots, x_{iD})^T \in R^D \tag{20}$$

$$v_i = (v_{i1}, v_{i2}, \ldots, v_{iD})^T \in R^D, i = 1, 2, \ldots, N \tag{21}$$

D refers to the number of decision variables, and the particle positions and velocities are updated as follows:

$$V_{id}^{t+1} = \omega V_{id}^t + c_1 r_1 \left(P_{id}^t - X_{id}^t\right) + c_2 r_2 \left(P_{gd}^t - X_{id}^t\right) \tag{22}$$

$$X_{id}^{t+1} = X_{id}^t + V_{id}^{t+1} \tag{23}$$

ω refers to the inertia weight; t refers to the iteration; $c_1, c_2 \geq 0$ refers to the acceleration coefficient, which is also known as the learning factor; r_1, r_2 refers to the random number between (0,1); P_{id}^t refers to the tth individual extreme value, which is called P-best; X_{id}^t refers to the tth self-position; P_{gd}^t refers to the tth swarm extreme value, which is called G-best. To balance the global search capability and local search capability of the particle swarm and improve search and solution speed, currently the most adopted is the dynamic, linear and changing inertia weight proposed by Shi (1988) [39], and the updated formula of inertia weight w is:

$$w = w_{max} - t \times \frac{w_{max} - w_{min}}{t_{max}} \tag{24}$$

In the formula: t refers to the current iteration; t_{max} refers to the maximum iteration. At the beginning of the iteration, setting a larger inertia weight is conducive to improving the global search capability; as the iteration increases, the inertia weight decreases, which is conducive to improving the local search capability for later iterations. In most applications, $w_{max} = 0.9, w_{min} = 0.4$.

4.1.2. Determine Individual Optimal Position and Global Optimal Position

Particles i and $i+1$ are the two appropriate solutions to the multi-objective optimization problem. If and only if Equation (25) is valid, we say that Particle i dominates Particle $i+1$.

$$\forall j = 1, 2, \ldots, f_j(i) \leq f_j(i+1) \wedge \exists j^* = 1, 2, \ldots, f_{j^*}(i) < f_{j^*}(i+1) \tag{25}$$

The Pareto dominant relationship is used to determine the optimal position of the particle. If the fitness value of the current particle is superior to P-best, the position of the current particle will be used to update P-best; otherwise, P-best will remain unchanged.

For the multi-objective optimization problem, the results of each iteration in the PSO algorithm will exclude the dominated particles, and use dominating particles and the particles that do not dominate each other to form a non-inferior solution set. Coello et al. (2004) defined the fitness value for the meshes divided in each swarm (containing at least one external particle), selected a mesh according to the roulette method and randomly screened an external particle swarm from the non-inferior solution set as the global extreme value [38].

4.2. TOPSIS Algorithm

According to the multi-objective PSO algorithm, the eventual result of the multi-objective optimization problem is a group of Pareto solution sets. Decision-makers need to screen the optimal compromise solution from the Pareto solution set, which in essence is a multi-property decision-making issue. The TOPSIS algorithm, also known as "Approximate Ideal Solution Ranking", is a decision-making method featuring multi-property decision-making analysis [40]. The relative nearness degree is obtained through calculating the distances from each solution to the optimal solution and the worst solution and used as the basis of evaluation.

Alternative solutions with the number of m are composed of elements in the Pareto solution set, which have corresponding function values under their own objectives for a multi-objective optimization problem with n objectives. The specific steps are as follows:

(1) Since the dimension and variation range of each objective are different, in order to reflect the actual situation that the objective changes with the decision variables, the z-score normalization method is adopted to perform de-dimension processing on objective functions;

(2) The entropy weight method is used to determine the weight λ_n of each objective;

(3) The optimal solution S^+ and the worst solution S^- are determined, that is to say, each objective has achieved the optimal and the worst solutions:

$$S^+ = \min\left(f_1{}'(x_1), f_2{}'(x_2), \ldots, f_n{}'(x_n)\right) \tag{26}$$

$$S^- = \max\left(f_1{}'(x_1), f_2{}'(x_2), \ldots, f_n{}'(x_n)\right) \tag{27}$$

(4) The distances from the solution x_i to the optimal solution and the worst solution are calculated, and thus the relative nearness degree d is calculated.

$$d_+(x_i) = \lambda_n \sqrt{\sum_{n=1}^{m} \left[f'_n(x_i) - f'_{n+}\right]^2} \tag{28}$$

$$d_+(x_i) = \lambda_n \sqrt{\sum_{n=1}^{m} \left[f'_n(x_i) - f'_{n+}\right]^2} \tag{29}$$

$$d(x_i) = \frac{d_+(x_i)}{d_+(x_i) + d_-(x_i)} \tag{30}$$

In the formula, the smaller the value of d, the closer the solution x_i is to the optimal solution; the minimum corresponding solution of d is the optimal compromise solution.

4.3. Solving Process

(1) The particle swarm is initialized to give each particle an initial speed and position. The learning factors c_1, c_2, the upper and lower limits of inertia weights w_{max} , w_{min}, the maximum iteration t_{max} as well as the particle swarm size N and other parameters are simultaneously initialized;

(2) The fitness value of the particle is calculated, which is determined by the function values of ship cost and carbon emissions, that is to say

$$\begin{cases} TC\left(v_i^E, v_i^N\right) = C_R + C_S + C_{co_2} + C_G \\ F_{co_2}\left(v_i^E, v_i^N\right) = F_{co_2} \end{cases} \tag{31}$$

After the algorithm is initialized and updated, the constraints specified by the two objective functions are satisfied by limiting the range of values of decision variables;

(3) The fitness of particles is compared, and the individual optimal position (P-best) and non-inferior solution set are updated according to the dominant relationship, and the global optimal position (G-best) of the particle is randomly selected from the non-inferior solution set;

(4) According to the particle update formula, the speed and position of the particles are updated to judge whether the particle is trapped in a local optimal solution. If so, it is necessary to mutate;

(5) It needs to judge whether the pre-set maximum iteration has been achieved, and output the Pareto solution set; otherwise, return to step (2) to continue the iteration;

(6) According to the obtained Pareto solution set, the corresponding minimum and maximum values of ship cost and emissions are found, which are the positive and negative ideal points;

(7) The solution with the minimum relative distance d from the positive and negative ideal points is screened from the solution set, which is the optimal compromise solution, and the corresponding speed is the optimal speed.

The specific flow chart of the solution is shown in Figure 3.

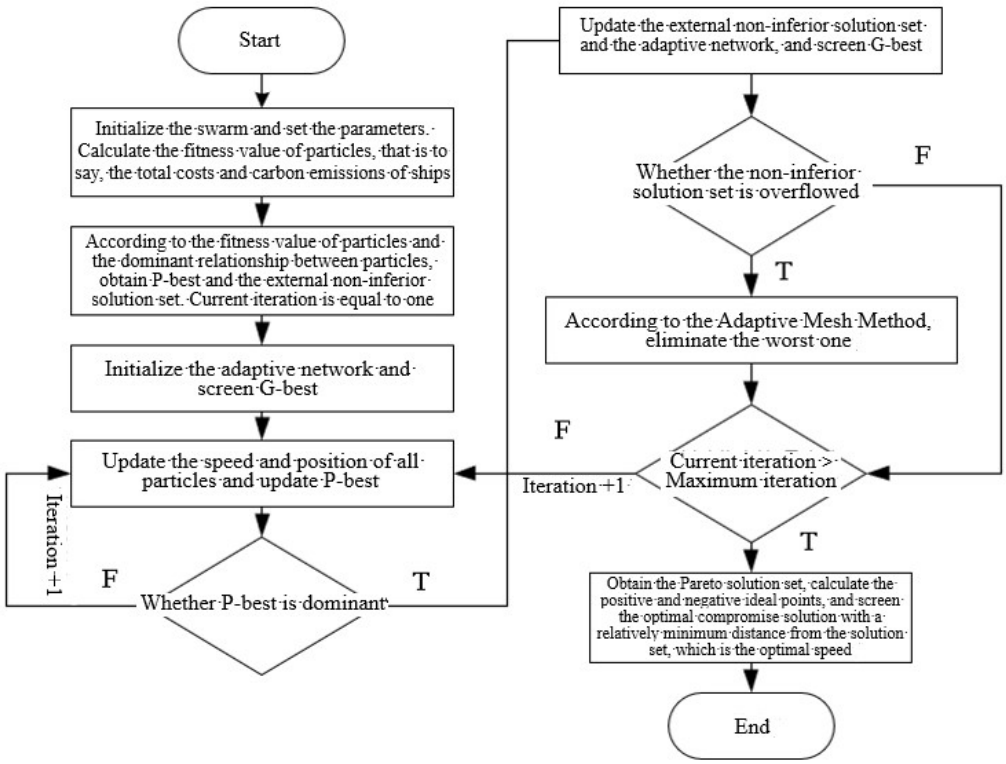

Figure 3. Flow chart of the solution.

5. Case Study

5.1. Route Profile

Based on the above-mentioned algorithms, this paper takes the regular weekly service of the trans-Pacific route provided by the liner carrier Yang Ming (the specific route is PACIFIC SOUTH WEST COAST LOOP4) as an example. The ports involved along this route are successively Hong Kong, Yantian, Kaohsiung, Keelung, Los Angeles, Oakland, Keelung, Kaohsiung and Hong Kong, with the ports of Los Angeles and Oakland providing AMP services. The specific distances between ports and the berthing time are shown in Table 2, among which the source of the total distance D_i between ports is SeaRates (www.searates.com accessed on 25 June 2022.). D_i^E is the distance for leg i in SECAs. D_i^N is the distance for leg i outside SECAs. Parameters related to ships are provided in Table 3 based on the relevant literature.

Table 2. Leg summary and AMP subsidy policies.

Leg$i$	Area	Total Distance D_i(n mile)	D_i^E (n mile)	D_i^N (n mile)	t_j (h)	P_j^{AMP} (USD/kWh)	B_j^{AMP} (USD/Cycle)
1	Hong Kong–Yantian	40.59	0	40.59	24		
2	Yantian–Kaohsiung	339.4	58.45	280.95	28.8		
3	Kaohsiung–Keelung	234.21	38	196.21	24		
4	Keelung–Los Angeles	5896.38	87	5809.38	24		
5	Los Angeles–Oakland	407.55	407.55	0	38.4	0.2	550
6	Oakland–Keelung	5633.21	69	5567.21	48	0.15	152
7	Keelung–Kaohsiung	234.21	38	196.21	24		
8	Kaohsiung–Hong Kong	345.22	71	274.22	24		

Table 3. Model parameters.

Sign	Value	Sign	Value
I	8	$f_{co_2}^E$	3.082
J	9	$f_{co_2}^N$	3.012
V_M (n mile)	25	F_F (t/d)	7.14
V_m (n mile)	10	Cg (USD/d)	22,000
P_{CO_2} (USD/t)	47	F_{FS} (t/d)	7.14
P_E (USD/t)	558	Q_{AMP} (kWh/t)	25,200
P_N (USD/t)	323	n	8

5.2. Result Analysis

In this paper, the specific relationships among speed, ship operating cost and carbon emissions are obtained. As shown in Figure 4, the blue line represents the relationship between ship operating cost and speed, and the red line shows the relationship between carbon emissions and speed. At a speed between 10 and 13.63, the ship speed is negatively correlated with operating cost while positively correlated with carbon emissions, that is to say, the two objectives are in conflict.

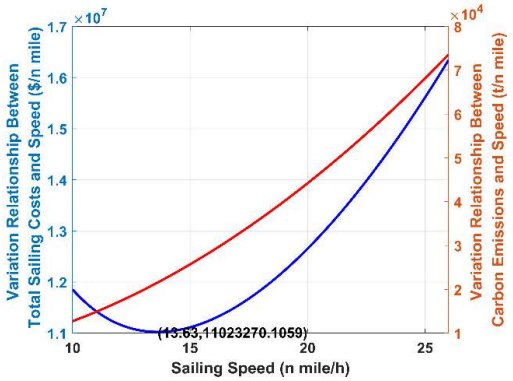

Figure 4. Relationship diagram of dual objectives and speed.

In order to obtain the approximate optimal solution of the example, the parameters of MOPSO were adjusted appropriately. The parameter values of MOPSO are the particle swarm size $N = 50$, the acceleration coefficient $c_1 = 1.5$, $c_2 = 0.5$, the maximum inertia weight $\omega_{max} = 1.2$, the minimum inertia weight $\omega_{min} = 0.2$, the maximum iteration $t_{max} = 100$ and the updating method of inertia weight which is as follows:

$$w = w_{max} - t \times \frac{w_{max} - w_{min}}{t_{max}}$$

According to the established multi-objective optimization algorithm of the ship, the simulation calculation is performed on the actual case, and the result is shown in Figure 5. The red asterisks represent the positions of 50 swarm-optimal particles after the 100th iteration, which have formed the Pareto solution set, while the white circles represent the positions of 50 particles in the 100th iteration. Table 4 shows the values of the dual objective function corresponding to 50 particles.

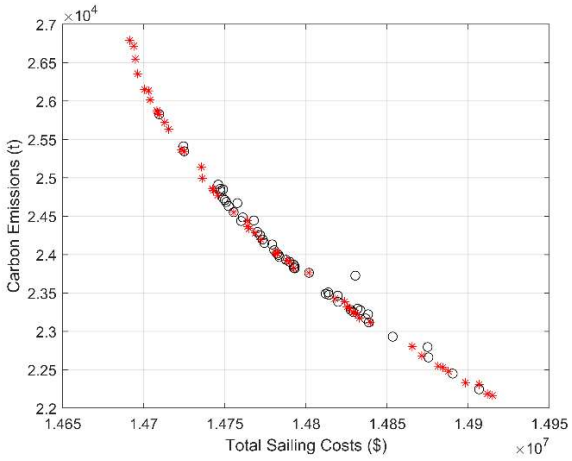

Figure 5. Pareto front for ship cost and emissions.

Table 4. 50 objective function values corresponding to Pareto solution.

No.	Cost (USD)	Carbon Emission (t)	No.	Cost (USD)	Carbon Emission (t)	No.	Cost (USD)	Carbon Emission (t)
1	14,694,000	26,943	18	14,744,000	24,846	35	14,739,000	25,024
2	14,712,000	25,940	19	14,721,000	25,588	36	14,812,000	23,512
3	14,699,000	26,532	20	14,707,000	25,988	37	14,775,000	24,188
4	14,743,000	24,907	21	14,692,000	27,094	38	14,838,000	23,112
5	14,891,000	22,421	22	14,745,000	24,829	39	14,765,000	24,411
6	14,696,000	26,544	23	14,757,000	24,586	40	14,879,000	22,547
7	14,896,000	22,335	24	14,737,000	25,100	41	14,775,000	24,203
8	14,876,000	22,589	25	14,765,000	24,411	42	14,794,000	23,876
9	14,909,000	22,183	26	14,887,000	22,455	43	14,787,000	23,976
10	14,711,000	25,987	27	14,695,000	26,810	44	14,873,000	22,617
11	14,905,000	22,229	28	14,914,000	22,159	45	14,835,000	23,145
12	14,861,000	22,771	29	14,713,000	25,931	46	14,854,000	22,911
13	14,822,000	23,346	30	14,762,000	24,486	47	14,845,000	22,999
14	14,780,000	24,148	31	14,777,000	24,161	48	14,804,000	23,665
15	14,781,000	24,057	32	14,900,000	22,303	49	14,807,000	23,592
16	14,706,000	26,108	33	14,727,000	25,377	50	14,829,000	23,251
17	14,759,000	24,504	34	14,863,000	22,750	—	—	—

The 50 particles obtained are used to form the Pareto solution set. The respective weights of the dual objectives are first determined through the entropy weight method. The formula of calculating information entropy is as follows:

$$E_i = -\frac{1}{\ln n} \sum_{j=1}^{n} p_{ij} \ln p_{ij} \quad (32)$$

where p_{ij} refers to the proportion of each item in the total, with i as the index, j as the number of records and E_i between 0 and 1.

The formula of calculating the weight of each index λ_i through information entropy is as follows:

$$\lambda_i = \frac{1 - E_i}{\sum(1 - E_i)} \tag{33}$$

The results of the respective weights of the dual objectives are shown in Table 5.

Table 5. Results of weights determined by entropy weight method.

Item	Information Entropy Value e	Information Utility Value d	Weight
Objective 1 (Cost)	0.951	0.049	0.563
Objective 2 (Carbon Emissions)	0.962	0.038	0.437

The TOPSIS algorithm is adopted and the weights of each objective obtained through the entropy weight method are combined to rank the Pareto solution set. The number of the selected optimal compromise solution (the optimal speed) is 18. The results of ranking are shown in Table 6.

Table 6. Results of TOPSIS method ranking.

No.	Positive Distance	Negative Distance	Comprehensive Score	Rank	No.	Positive Distance	Negative Distance	Comprehensive Score	Rank
18	0.0869	0.1437	0.6231	1	49	0.0961	0.1294	0.5737	25
22	0.0868	0.1433	0.6227	2	36	0.0986	0.1289	0.5666	26
17	0.0845	0.1388	0.6216	3	6	0.1266	0.1652	0.5661	27
4	0.0882	0.1436	0.6196	4	3	0.1263	0.1630	0.5633	28
23	0.0855	0.1388	0.6188	5	13	0.1039	0.1285	0.5530	29
35	0.0900	0.1449	0.6169	6	27	0.1343	0.1654	0.5519	30
30	0.0854	0.1372	0.6162	7	1	0.1381	0.1660	0.5459	31
25	0.0852	0.1365	0.6157	8	50	0.1080	0.1281	0.5425	32
39	0.0852	0.1365	0.6157	8	21	0.1425	0.1675	0.5404	33
24	0.0914	0.1454	0.6139	9	45	0.1116	0.1286	0.5355	34
37	0.0857	0.1343	0.6103	10	38	0.1135	0.1284	0.5308	35
41	0.0860	0.1340	0.6090	11	47	0.1179	0.1292	0.5227	36
33	0.0966	0.1495	0.6076	12	46	0.1241	0.1289	0.5095	37
31	0.0863	0.1336	0.6075	13	12	0.1287	0.1310	0.5045	38
15	0.0867	0.1332	0.6059	14	34	0.1301	0.1312	0.5020	39
14	0.0878	0.1321	0.6008	15	44	0.1372	0.1329	0.4920	40
19	0.1014	0.1519	0.5998	16	8	0.1394	0.1332	0.4886	41
43	0.0888	0.1314	0.5968	17	40	0.1415	0.1339	0.4862	42
20	0.1111	0.1594	0.5892	18	26	0.1473	0.1354	0.4790	43
42	0.0915	0.1297	0.5863	19	5	0.1503	0.1360	0.4750	44
2	0.1102	0.1560	0.5860	20	7	0.1540	0.1380	0.4727	45
29	0.1100	0.1553	0.5853	21	32	0.1570	0.1387	0.4691	46
10	0.1114	0.1564	0.5840	22	11	0.1607	0.1406	0.4667	47
16	0.1145	0.1595	0.5821	23	9	0.1637	0.1418	0.4642	48
48	0.0950	0.1292	0.5762	24	28	0.1675	0.1425	0.4596	49

Table 7 shows that, except for the Yantian–Kaohsiung section, the sailing speed in ECA is less than that outside ECA. The results show that the establishment of ECA can effectively reduce ship speed and carbon emission. At the same time, the longer the navigation distance of the segment, the faster the speed outside the control area, which compensates for the time loss caused by the active speed reduction in the ECA area and satisfies the service frequency. Finally, with fixed fuel prices, the faster speed outside the ECA will increase fuel costs, but also substantially reduce fixed daily costs. Tables 8 and 9 show the single-objective optimization results with minimum sailing cost and minimum CO_2 emission. By comparing the optimization results in Tables 7 and 8, the sailing speed of the double-objective optimization is significantly lower than that of the single-objective optimization with the minimum sailing cost, so the CO_2 emission decreases but the cost increases. By comparing the optimization results in Tables 7 and 9, the sailing speed of the double-objective optimization is higher than that of the single-objective optimization with the minimum CO_2 emission, so the sailing cost decreases but the carbon emission increases.

Table 7. Results of multi-objective optimization of speed.

Leg$i$	Area	Total Distance D_i (n mile)	D_i^E (n mile)	v_i^E (n mile/h)	D_i^N (n mile)	v_i^N (n mile/h)
1	Hong Kong–Yantian	40.59	0	—	40.59	12.07
2	Yantian–Kaohsiung	339.4	58.45	12.16	280.95	11.79
3	Kaohsiung–Keelung	234.21	38	11.71	196.21	12.60
4	Keelung–Los Angeles	5896.38	87	11.61	5809.38	12.81
5	Los Angeles–Oakland	407.55	407.55	11.73	0	—
6	Oakland–Keelung	5633.21	69	11.66	5567.21	12.68
7	Keelung–Kaohsiung	234.21	38	11.49	196.21	12.38
8	Kaohsiung–Hong Kong	345.22	71	11.45	274.22	12.09

Table 8. Results of minimum sailing cost of speed.

Leg$i$	Area	Total Distance D_i (n mile)	D_i^E (n mile)	v_i^E (n mile/h)	D_i^N (n mile)	v_i^N (n mile/h)
1	Hong Kong–Yantian	40.59	0	—	40.59	12.79
2	Yantian–Kaohsiung	339.4	58.45	10.93	280.95	11.47
3	Kaohsiung–Keelung	234.21	38	11.78	196.21	12.41
4	Keelung–Los Angeles	5896.38	87	11.30	5809.38	13.25
5	Los Angeles–Oakland	407.55	407.55	11.79	0	—
6	Oakland–Keelung	5633.21	69	12.59	5567.21	13.19
7	Keelung–Kaohsiung	234.21	38	11.95	196.21	11.43
8	Kaohsiung–Hong Kong	345.22	71	12.18	274.22	13.53

Table 9. Results of minimum CO_2 emissions of speed.

Leg$i$	Area	Total Distance D_i (n mile)	D_i^E (n mile)	v_i^E (n mile/h)	D_i^N (n mile)	v_i^N (n mile/h)
1	Hong Kong–Yantian	40.59	0	—	40.59	12.45
2	Yantian–Kaohsiung	339.4	58.45	11.41	280.95	11.52
3	Kaohsiung–Keelung	234.21	38	11.57	196.21	12.67
4	Keelung–Los Angeles	5896.38	87	11.35	5809.38	11.71
5	Los Angeles–Oakland	407.55	407.55	11.82	0	—
6	Oakland–Keelung	5633.21	69	11.40	5567.21	12.08
7	Keelung–Kaohsiung	234.21	38	12.01	196.21	11.13
8	Kaohsiung–Hong Kong	345.22	71	11.89	274.22	11.53

The results in Table 10 show that, with speed optimization, the ship's carbon emissions correspond to 24,846 tons. Compared to the objective of minimizing carbon emissions, carbon emissions are increased by 2200 tons; however, the total ship costs are reduced by USD 170,000, showing a significant effect. The main reason is that the optimized speed is relatively faster which increases carbon emissions but significantly reduces sailing time, thus reducing the fixed cost and the total costs. Meanwhile, compared to the objective of minimizing total costs, carbon emissions were reduced by 2200 tons; however, the total ship costs only increased by USD 50,000. The above-mentioned results show that this speed optimization algorithm has a certain advantage. This algorithm can provide references for ships to determine the speed and reduce costs in optimizing speed, taking into account economic and environmental benefits in the process of ship operation.

Table 10. A comparison of various emission control policies.

Strategy Considered	Minimum TC	Minimum F_{CO_2}	Optimal TC and F_{CO_2}
Total Cost TC (USD 10,000)	1469.2	1491.4	1474.4
Fuel Cost C_R (USD 10,000)	409.6	370.53	393.31
Emission Cost C_{CO_2} (USD 10,000)	127.4	104.14	117.9
Sailing Time T (h)	992.9	1108.1	1039.5
Carbon Emission F_{CO_2} (t)	27094	22,159	24,846

6. Conclusions

In a sustainable developing society, ship operating cost optimization and carbon emission reduction are key goals of the transportation industry. There is a dilemma

between ship operating cost and carbon emission reduction. A major part of the solution is to take advantage of the growing technologies and operational strategies to increase ship efficiency. This paper establishes a ship speed dual-objective optimization model taking into consideration the impacts of the ECA control area, berthing cost and AMP, adopting the multi-objective PSO algorithm to find the Pareto solution set with the dual objectives of minimizing ship operating cost and carbon emission, using the TOPSIS algorithm to screen the optimal compromise solution from the Pareto solution set and finding the optimal speeds for various legs. Taking the Yang Ming route as an example, we perform simulation calculations with the established model. The results show that our model can effectively find the optimal compromise speed. By increasing speed, the dual objectives of total ship costs and ship carbon emissions can be effectively balanced. This can achieve the balance objective of sustaining economic development and protecting the environment.

In this paper, the minimization of shipping cost is regarded as one of the optimization objectives. For future work, considering the maximization of shipping profit as an optimization object, the multi-objective optimization model including carbon emission, profit maximization and other factors can be constructed to fit the actual operation of shipping companies.

Author Contributions: Conceptualization, X.W. and Y.W.; methodology and software, J.L.; validation, X.W., Y.W. and J.L.; formal analysis, J.L.; investigation, J.L.; funding acquisition, X.W. All authors have read and agreed to the published version of the manuscript.

Funding: This research was funded by [the National Social Science Foundation of China] grant number [18ZDA052].

Institutional Review Board Statement: The authors exclude this statement.

Informed Consent Statement: The authors exclude this statement.

Data Availability Statement: Publicly available datasets were analyzed in this study. This data can be found here: [https://www.cnss.com.cn/ and www.searates.com].

Conflicts of Interest: The authors declare no conflict of interest.

References

1. Shi, K.; Weng, J.; Li, G. Exploring the Effectiveness of ECA Policies in Reducing Pollutant Emissions from Merchant Ships in Shanghai Port Waters. *Mar. Pollut. Bull.* **2020**, *155*, 111164. [CrossRef] [PubMed]
2. Wu, X.; Deng, H.; Huang, Y.; Guo, J. Air Pollution, Migration Costs, and Urban Residents' Welfare: A Spatial General Equilibrium Analysis from China. *Struct. Chang. Econ. Dyn.* **2022**, *63*, 396–409. [CrossRef]
3. Wu, X.; Tian, Z.; Kuai, Y.; Song, S.; Marson, S.M. Study on Spatial Correlation of Air Pollution and Control Effect of Development Plan for the City Cluster in the Yangtze River Delta. *Socioecon. Plann. Sci.* **2022**, *83*, 101213. [CrossRef]
4. Jing, D.; Dai, L.; Hu, H.; Ding, W.; Wang, Y.; Zhou, X. CO_2 Emission Projection for Arctic Shipping: A System Dynamics Approach. *Ocean Coast. Manag.* **2021**, *205*, 105531. [CrossRef]
5. Xu, H.; Yang, D. LNG-Fuelled Container Ship Sailing on the Arctic Sea: Economic and Emission Assessment. *Transp. Res. D Transp. Environ.* **2020**, *87*, 102556. [CrossRef]
6. Lin, G.H.; Liang, R.N.; Li, Y.W.; Xu, W.N. Optimal Strategies for Liner Shipping Considering Integrated Emission Reduction Strategies. *Ind. Eng. Manag.* **2022**, *27*, 83–93.
7. Lashgari, M.; Akbari, A.A.; Nasersarraf, S. A New Model for Simultaneously Optimizing Ship Route, Sailing Speed, and Fuel Consumption in a Shipping Problem under Different Price Scenarios. *Appl. Ocean Res.* **2021**, *113*, 102725. [CrossRef]
8. Fan, A.; Wang, Z.; Yang, L.; Wang, J.; Vladimir, N. Multi-Stage Decision-Making Method for Ship Speed Optimization Considering Inland Navigational Environment. *Proc. Inst. Mech. Eng. Part M J. Eng. Marit. Environ.* **2021**, *235*, 372–382. [CrossRef]
9. Li, X.; Sun, B.; Guo, C.; Du, W.; Li, Y. Speed Optimization of a Container Ship on a given Route Considering Voluntary Speed Loss and Emissions. *Appl. Ocean Res.* **2020**, *94*, 101995. [CrossRef]
10. Gao, C.-F.; Hu, Z.-H. Speed Optimization for Container Ship Fleet Deployment Considering Fuel Consumption. *Sustainability* **2021**, *13*, 5242. [CrossRef]
11. Wang, S.; Zhao, Q. Probabilistic Tabu Search Algorithm for Container Liner Shipping Problem with Speed Optimization. *Int. J. Prod. Res.* **2022**, *60*, 3651–3668. [CrossRef]
12. Yu, B.; Peng, Z.; Tian, Z.; Yao, B. Sailing Speed Optimization for Tramp Ships with Fuzzy Time Window. *Flex. Serv. Manuf. J.* **2019**, *31*, 308–330. [CrossRef]

13. Doudnikoff, M.; Lacoste, R. Effect of a Speed Reduction of Containerships in Response to Higher Energy Costs in Sulphur Emission Control Areas. *Transp. Res. D Transp. Environ.* **2014**, *28*, 51–61. [CrossRef]
14. Ng, M. Vessel Speed Optimisation in Container Shipping: A New Look. *J. Oper. Res. Soc.* **2019**, *70*, 541–547. [CrossRef]
15. De, A.; Choudhary, A.; Turkay, M.; Tiwari, M.K. Bunkering Policies for a Fuel Bunker Management Problem for Liner Shipping Networks. *Eur. J. Oper. Res.* **2021**, *289*, 927–939. [CrossRef]
16. De, A.; Kumar, S.K.; Gunasekaran, A.; Tiwari, M.K. Sustainable Maritime Inventory Routing Problem with Time Window Constraints. *Eng. Appl. Artif. Intell.* **2017**, *61*, 77–95. [CrossRef]
17. Dulebenets, M.A. Green Vessel Scheduling in Liner Shipping: Modeling Carbon Dioxide Emission Costs in Sea and at Ports of Call. *Int. J. Transp. Sci. Technol.* **2018**, *7*, 26–44. [CrossRef]
18. Zis, T.; North, R.J.; Angeloudis, P.; Ochieng, W.Y.; Harrison Bell, M.G. Evaluation of Cold Ironing and Speed Reduction Policies to Reduce Ship Emissions near and at Ports. *Marit. Econ. Logist.* **2014**, *16*, 371–398. [CrossRef]
19. Tang, R.; Wu, Z.; Li, X. Optimal Operation of Photovoltaic/Battery/Diesel/Cold-Ironing Hybrid Energy System for Maritime Application. *Energy* **2018**, *162*, 697–714. [CrossRef]
20. Lan, X.; Zuo, X.; Tang, X. The Impact of Different Carbon Emission Policies on Liner Shipping. *J. Mar. Sci.* **2020**, *2020*, 1–12. [CrossRef]
21. De, A.; Mamanduru, V.K.R.; Gunasekaran, A.; Subramanian, N.; Tiwari, M.K. Composite Particle Algorithm for Sustainable Integrated Dynamic Ship Routing and Scheduling Optimization. *Comput. Ind. Eng.* **2016**, *96*, 201–215. [CrossRef]
22. Ding, W.; Wang, Y.; Dai, L.; Hu, H. Does a Carbon Tax Affect the Feasibility of Arctic Shipping? *Transp. Res. D Transp. Environ.* **2020**, *80*, 102257. [CrossRef]
23. De, A.; Wang, J.; Tiwari, M.K. Hybridizing Basic Variable Neighborhood Search with Particle Swarm Optimization for Solving Sustainable Ship Routing and Bunker Management Problem. *IEEE Trans. Intell. Transp. Syst.* **2020**, *21*, 986–997. [CrossRef]
24. Xing, Y.; Yang, H.; Ma, X.; Zhang, Y. Optimization of Ship Speed and Fleet Deployment under Carbon Emissions Policies for Container Shipping. *Transport* **2019**, *34*, 260–274. [CrossRef]
25. De, A.; Wang, J.; Tiwari, M.K. Fuel Bunker Management Strategies within Sustainable Container Shipping Operation Considering Disruption and Recovery Policies. *IEEE Trans. Eng. Manag.* **2021**, *68*, 1089–1111. [CrossRef]
26. Fan, H.; Yu, J.; Liu, X. Tramp Ship Routing and Scheduling with Speed Optimization Considering Carbon Emissions. *Sustainability* **2019**, *11*, 6367. [CrossRef]
27. Zhen, L.; Hu, Z.; Yan, R.; Zhuge, D.; Wang, S. Route and Speed Optimization for Liner Ships under Emission Control Policies. *Transp. Res. Part C Emerg. Technol.* **2020**, *110*, 330–345. [CrossRef]
28. Christodoulou, A.; Gonzalez-Aregall, M.; Linde, T.; Vierth, I.; Cullinane, K. Targeting the Reduction of Shipping Emissions to Air: A Global Review and Taxonomy of Policies, Incentives and Measures. *Marit. Bus. Rev.* **2019**, *4*, 16–30. [CrossRef]
29. Liu, H.; Fu, M.; Jin, X.; Shang, Y.; Shindell, D.; Faluvegi, G.; Shindell, C.; He, K. Health and Climate Impacts of Ocean-Going Vessels in East Asia. *Nat. Clim. Chang.* **2016**, *6*, 1037–1041. [CrossRef]
30. Burel, F.; Taccani, R.; Zuliani, N. Improving Sustainability of Maritime Transport through Utilization of Liquefied Natural Gas (LNG) for Propulsion. *Energy* **2013**, *57*, 412–420. [CrossRef]
31. Ju, Y.; Hargreaves, C.A. The Impact of Shipping CO_2 Emissions from Marine Traffic in Western Singapore Straits during COVID-19. *Sci. Total Environ.* **2021**, *789*, 148063. [CrossRef] [PubMed]
32. Hughes, C.N. *Ship Performance: Technical, Safety, Environmental and Commercial Aspects*, 2nd ed.; Lloyd'S of London Press: London, UK, 1996; ISBN 978-1859780695.
33. Xue, Y.X.; Shao, J.G. Fleet Deployment for Liner Shipping in Low-Carbon Economy. *Navig. China* **2014**, *37*, 115–119.
34. De, A.; Choudhary, A.; Tiwari, M.K. Multiobjective Approach for Sustainable Ship Routing and Scheduling with Draft Restrictions. *IEEE Trans. Eng. Manag.* **2019**, *66*, 35–51. [CrossRef]
35. Peng, Y.; Dong, M.; Li, X.; Liu, H.; Wang, W. Cooperative Optimization of Shore Power Allocation and Berth Allocation: A Balance between Cost and Environmental Benefit. *J. Clean. Prod.* **2021**, *279*, 123816. [CrossRef]
36. Mandal, P.; Mondal, S.C. Multi-Objective Optimization of Cu-MWCNT Composite Electrode in Electro Discharge Machining Using MOPSO-TOPSIS. *Measurement* **2021**, *169*, 108347. [CrossRef]
37. Kennedy, J.; Eberhart, R. Particle Swarm Optimization. In Proceedings of the ICNN'95—International Conference on Neural Networks, Perth, Australia, 27 November–1 December 1995; IEEE: Piscataway, NJ, USA, 2002.
38. Coello, C.A.C.; Pulido, G.T.; Lechuga, M.S. Handling Multiple Objectives with Particle Swarm Optimization. *IEEE Trans. Evol. Comput.* **2004**, *8*, 256–279. [CrossRef]
39. Shi, Y.; Eberhart, R. A Modified Particle Swarm Optimizer. In Proceedings of the 1998 IEEE International Conference on Evolutionary Computation Proceedings, Anchorage, AK, USA, 4–9 May 2022; IEEE World Congress on Computational Intelligence (Cat. No.98TH8360). IEEE: Piscataway, NJ, USA, 2002.
40. Hwang, C.L.; Yoon, K. *Methods for Multiple Attribute Decision Making*; Springer: Berlin, Germany, 1981; pp. 58–191. ISBN 978-3-540-10558-9. [CrossRef]